Synthesis, Characterization, and Thermophysical Evaluation of MgO Nanoparticles and Their Nanofluids Prepared via the Sol-Gel Method

Mahesh T. Kotkar^{1*}, Subhash M. Wani², Pooja G. Shinde¹, A. G. Patil³, K. M. Jadhav⁴

¹PG Department of Physics and Research Center, Deogiri College, Chhatrapati Sambhajinagar (Aurangabad) - 431004 (M.S.), India ²Department of Physics, R. G. Bagdia Arts, S. B. Lakhotia Commerce and R. Benzoji Science College, Jalna - 431 203 (M.S.), India ³Department of Physics, Vivekanand Arts, Sardar Dalipsingh Commerce and Science College Chhatrapati Sambhajinagar (Aurangabad) - 431 001 (M.S.), India

⁴School of Basic and Applied Sciences, MGM University, Chhatrapati Sambhajinagar (Aurangabad) - 431 003, (M.S.), India

*Corresponding author email: maheshpatil4044@gmail.com

Abstract

This study focuses on the synthesis and characterization of magnesium oxide (MgO) nanoparticles prepared via the sol–gel method. The structural, functional, and optical properties of the synthesized MgO nanoparticles were analyzed using X-ray diffraction (XRD), Fourier-transform infrared spectroscopy (FTIR), and ultraviolet–visible (UV–Vis) spectroscopy techniques. XRD analysis confirmed the formation of well-defined crystalline MgO nanoparticles with uniform crystallite size. FTIR spectra exhibited characteristic peaks corresponding to the asymmetric and symmetric stretching vibrations of Mg–O bonds, confirming the successful formation of MgO. The UV–Vis spectrum revealed a broad and prominent excitonic absorption band in the range of 260–300 nm, indicating the nanoscale nature of the particles. The optical band gap of the synthesized MgO nanoparticles was estimated to be 3.14 eV, consistent with the semiconductor behaviour of nanosized MgO. The prepared MgO nanofluids were evaluated for their thermophysical properties. The viscosity of the MgO–deionized water nanofluids was measured using an Ostwald viscometer, while the thermal conductivity was estimated based on the Maxwell model. The stability of the nanofluids was assessed through zeta potential analysis. The results demonstrate that MgO nanoparticles synthesized via the sol–gel route possess high crystallinity, excellent stability, and predominantly nano spherical morphology, making them suitable for heat transfer and fluid dynamic applications.

Keywords: MgO nanoparticles, sol-gel method, XRD, FTIR, UV-vis, thermal conductivity.

Introduction

Metal oxide nanoparticles have received significant attention in recent years due to their unique physical and chemical properties compared to their bulk counterparts [1]. Among them, magnesium oxide (MgO) nanoparticles have emerged as a promising material because of their wide band gap, high melting point, chemical stability, and excellent catalytic and optical properties [2, 3]. These characteristics make MgO

nanoparticles suitable for a variety of applications such as catalysts, sensors, antibacterial agents, refractory materials, and in electronic and optical devices [4].

ISSN: 2582-3930

The properties of MgO nanoparticles strongly depend on their particle size, morphology, and crystallinity, which are influenced by the synthesis method [5]. Various methods, such as co-precipitation, hydrothermal, sol-gel, and combustion techniques, have been used to synthesize MgO nanoparticles [6, 7]. Among these, the sol-gel method is preferred because it allows better control over composition, homogeneity, and particle size at relatively low temperatures [8].

Characterization plays an important role in understanding the structure and properties of synthesized nanoparticles. X-ray diffraction (XRD) is used to determine the crystalline structure and average crystallite size of the MgO nanoparticles [9, 10]. Fourier-transform infrared spectroscopy (FTIR) provides information about the bonding and functional groups, confirming the formation of Mg–O bonds [11, 12]. Ultraviolet–visible (UV– Vis) spectroscopy helps in studying the optical properties, particularly the absorption characteristics related to the electronic transitions in the material [13, 14].

The structural, functional, and optical properties were systematically analyzed to confirm the formation and purity of MgO nanoparticles and to understand their suitability for further applications [15, 16].

Furthermore, MgO nanoparticles were dispersed in deionized water to prepare MgO-based nanofluids at different volume concentrations [17]. The stability, thermal, and rheological properties of these nanofluids were investigated to evaluate their potential for heat transfer and fluid dynamic applications [18, 19]. The zeta potential of the MgO nanofluids was measured to assess their colloidal stability, as a higher zeta potential value indicates better dispersion and reduced particle aggregation [20, 21]. The thermal conductivity of the nanofluids was measured using a maxwell model thermal property analyzer to examine the enhancement in heat transfer characteristics with varying nanoparticle concentrations [22, 23]. Additionally, the viscosity of the MgO nanofluids was determined using an Ostwald viscometer to understand the flow behaviour and its dependence on temperature and concentration [24, 25]. These analyses provide critical insights into the thermophysical behaviour and stability of MgO nanofluids, which are essential for their practical use in thermal management systems.

Method and materials

Synthesis of MgO NPs

Magnesium oxide (MgO) nanoparticles were synthesized using the sol-gel method. All the chemicals used were of analytical grade and were utilized without further purification. Magnesium nitrate hexahydrate Mg(NO₃)₂·6H₂O (Loba Chemie, India) was used as the magnesium precursor, and citric acid (C₆H₈O₇) served as the fuel and chelating agent.

For the synthesis, magnesium nitrate and citric acid were taken in a molar ratio of 1:1.5 and dissolved in 200 mL of deionized (DI) water under continuous magnetic stirring. The pH of the solution was adjusted to 8–9 using dilute ammonia solution. The mixture was stirred at 300 rpm and maintained at a temperature of 90 °C for approximately 3 hours until a homogeneous gel was formed, the obtained gel was then dried at 110 °C to

https://ijsrem.com © 2025, IJSREM DOI: 10.55041/IJSREM53580 Page 2



Volume: 09 Issue: 11 | Nov - 2025 SJIF Rating: 8.586 **ISSN: 2582-3930**

remove excess moisture, leading to the formation of a dry ash. The dried mass was subsequently sintered at 400 °C for 2 h in a muffle furnace to obtain the final MgO nanoparticles. Fig. 1. depicts flow chart of synthesis of MgO nanoparticles using sol-gel auto combustion method.

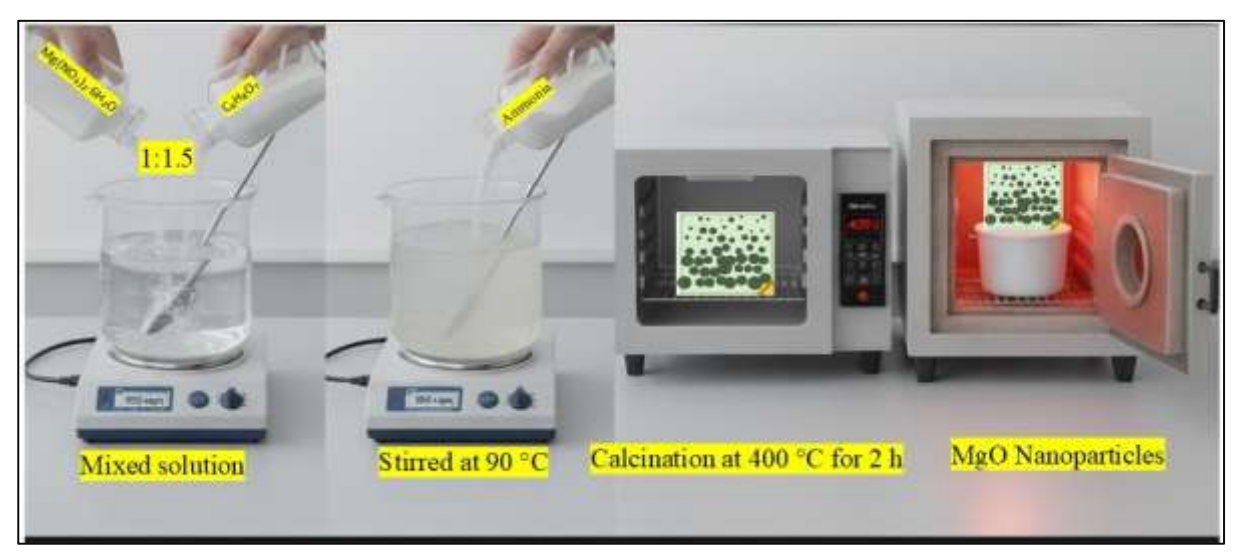


Fig.1. Schematic representation synthesis process of MgO NPs.

Preparation of MgO Nanofluids

Magnesium oxide (MgO) nanofluids were prepared by dispersing MgO nanoparticles in deionized (DI) water as the base fluid. Nanofluids with various volume concentrations of 0.020%, 0.040%, 0.060%, 0.080%, and 0.1% were formulated. For each concentration, 100 mL of DI water was used. The required amount of MgO nanoparticles was accurately weighed and gradually added to the DI water under continuous magnetic stirring to ensure uniform dispersion. The initially mixed suspension was subjected to probe sonication for 1 hour to break down any nanoparticle agglomerates and promote homogeneous dispersion. This was followed by bath sonication for 30 minutes to further stabilize the suspension and achieve uniform distribution of nanoparticles within the base fluid. The prepared MgO nanofluids were then allowed to cool to room temperature and stored in airtight containers for subsequent measurements and characterization. Fig.2.shows the nanofluids preparation process. Fig.3. Prepaed MgO – DI water nanofluids.

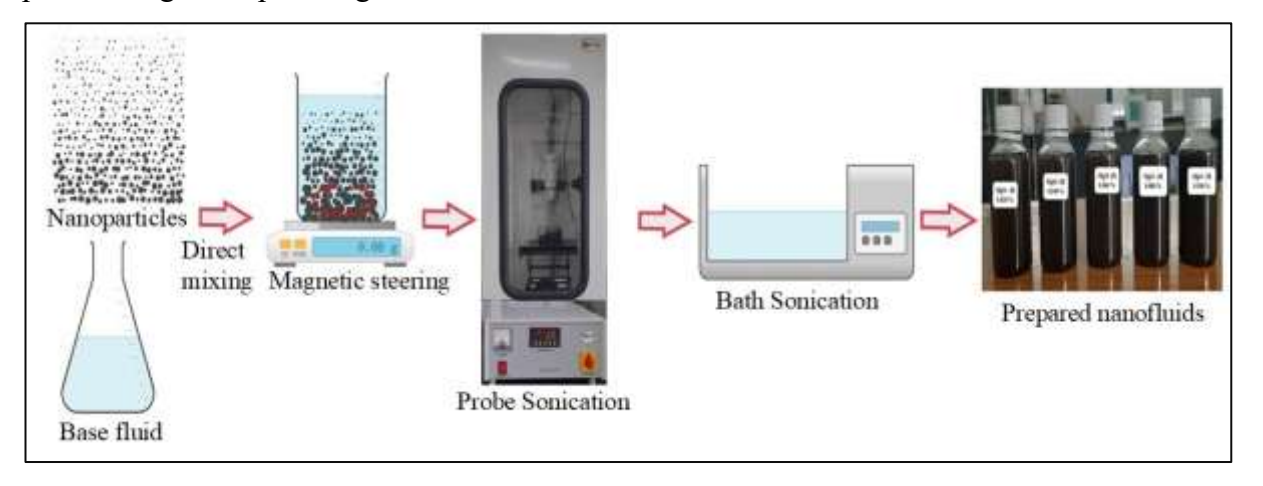


Fig.2. Nanofluids preparation process.

Volume: 09 Issue: 11 | Nov - 2025 SJIF Rating: 8.586 ISSN: 2582-3930



Fig.3. Prepaed MgO – DI water nanofluids.

Characterizations

The MgO nanoparticles (MgO NPs) were subjected to comprehensive structural and optical characterization using X-ray diffraction (XRD), Fourier-transform infrared spectroscopy (FTIR), and ultraviolet–visible (UV–Vis) spectroscopy. XRD analysis was performed using a Bruker D8 Advance diffractometer equipped with Cu-K α radiation (λ = 1.5406 Å), with scanning conducted over a 2 θ range of 15°–85° and a step size of 0.02°. This analysis was employed to determine the crystalline structure, phase purity, and average crystallite size of the synthesized MgO nanoparticles. FTIR spectroscopy was carried out using a Perkin-Elmer spectrometer in the wavenumber range of 400–4000 cm⁻¹ to identify the functional groups and confirm the metal–oxygen bonding in the samples. The optical characteristics of the MgO NPs were analyzed using a UV–Vis spectrophotometer (UV-2700i Plus) within the wavelength range of 200–800 nm to evaluate their optical absorption behaviour and estimate the band gap energy. The viscosity of MgO nanofluids was measured using an Ostwald viscometer, while the zeta potential was analyzed using a (Malvern Zeta sizer) to assess the stability of the suspension. The thermal conductivity of the nanofluids was evaluated using the Maxwell model.

Results and Discussion

X-ray Diffraction (XRD) Analysis

The X-ray Diffraction (XRD) pattern of MgO nanoparticles (NPs) is shown in Fig.4. The XRD pattern exhibits distinct diffraction peaks corresponding to the (111), (200), (220), (311), and (222) crystal planes, confirming the formation of a single-phase cubic periclase structure of MgO. The pattern well matches with JCPDS card no. 45-0946. The sharp and intense diffraction peaks indicate high crystallinity of the MgO nanoparticles. The absence of additional impurity peaks further confirms the phase purity of the synthesized MgO. Based on the structural analysis of the XRD data, the MgO NPs exhibit a cubic structure.

The lattice parameters (a, b, c) were calculated using the appropriate crystallographic relationships [15].

$$a = d\sqrt{h^2 + k^2 + l^2} \tag{1}$$

Here, the lattice parameters are given by a, b, and c, and (h k l) refers to the Miller indices of the crystal planes. The XRD analysis show cubic spinel structure, hence a = b = c The lattice parameters were listed in Table 1, which demonstrates that these parameters are in close agreement with the reported literature values.

The average crystallite size (D) was calculated using the Debye–Scherrer equation [26]:

$$D = \frac{K\lambda}{\beta \cos \theta} \tag{2}$$

where K is the shape factor (0.9), λ is the X-ray wavelength (1.5406 Å for Cu K α radiation), β is the full width at half maximum (FWHM) of the diffraction peak, and θ is the Bragg angle. The calculated average crystallite size was found to be in the nanometer range, indicating successful synthesis of MgO nanoparticles with good crystallinity.

Dislocation density (δ):

Dislocation density was calculated by using following formula [27],

$$\delta = \frac{1}{D^2} \tag{3}$$

where, D denotes the crystallite size in nm.

Lattice strain (LS):

Lattice strain was calculated by using following relation [28],

$$LS = \frac{\beta}{4\tan\theta} \tag{4}$$

Where β is the FWHM of the highest intensity peak and θ represents the angle of diffracted radiation.

Staking fault:

following relation was used to calculate staking fault [28],

$$(SF) = \frac{2\pi^2}{45\sqrt{3\tan\theta}} \tag{5}$$

The symbol θ represents the angle of the diffracted radiation in the X-ray diffraction process.

The values of various structural parameters such as dislocation density, lattice strain and staking fault were obtained utilizing the above equations and are mentioned in Table.2. The obtained parameters are dependent on crystallite size and the angle of diffracted radiation and are in reported range.

Volume: 09 Issue: 11 | Nov - 2025



SJIF Rating: 8.586

ISSN: 2582-3930

20000 - (in: 15000 - (in: 1500

Fig. 4. X-ray diffraction pattern of MgO nanoparticles.

Table.1. Values of Millar indices (hkl), Bragg's angle (2θ), Intensity (I), Interplanar spacing (d), lattice constant (a), crystallite size (D) for XRD pattern of MgO nanoparticles.

(hkl)	2θ	I	d	a, b and c	D
	(degree)	(a.u.)	(Å)	(Å)	(nm)
(200)	42.81	13177.41	2.11	a = b = c = 4.22	7.83

Table.2. Values of Molecular weight (M), Lattice strain (LS), Dislocation density (δ), Microstrain (ϵ), Staking fault (SF).

(hkl)	Mol. weight g/mol	LS* 10 ⁻³	δ * 10 ¹⁵ (lines/m²)	ε * 10 ⁻³	SF
(200)	40.30	12.12	16.30	4.42	0.4041

Fourier Transform Infrared (FTIR) Analysis

The FTIR spectrum of the synthesized magnesium oxide (MgO) nanoparticles, shown in Fig.5, reveals several distinct absorption bands corresponding to various vibrational modes. A broad absorption peak observed around 3411 cm⁻¹ is attributed to the O–H stretching vibration of surface-adsorbed water molecules or hydroxyl groups present on the nanoparticle surface. The moderate peak at 1515 cm⁻¹ corresponds to the bending vibration of H–O–H groups, further confirming the presence of adsorbed moisture. The characteristic absorption band appearing at 444 cm⁻¹ is assigned to the Mg–O stretching vibration, which confirms the successful formation of MgO nanoparticles. The absence of other significant impurity peaks indicates the high purity and successful synthesis of MgO.

SJIF Rating: 8.586

ISSN: 2582-3930

Volume: 09 Issue: 11 | Nov - 2025

20

4000

100 - % 80 - 60 - 40 - 3411

2000

Wavenumber (cm⁻¹)

1500

1000

500

Fig. 5. FTIR spectra of MgO nanoparticles.

2500

3000

3500

UV-Visible Spectroscopy

The UV-Vis absorbance spectrum of the MgO (magnesium oxide) nanoparticles, as shown in the Fig.6 (a), displays a prominent absorption peak around 300–330 nm, indicating strong absorption in the ultraviolet region. This peak is attributed to the intrinsic band gap absorption of MgO nanoparticles, which typically arises due to electronic transitions between the valence and conduction bands. The observed shift and shape of the peak may also be influenced by quantum confinement effects and surface defects, which are more pronounced at the nanoscale. The gradual decrease in absorbance beyond the UV region and minimal absorption in the visible range confirm that MgO nanoparticles are optically transparent in the visible region and have a wide band gap, making them suitable for applications in UV-blocking materials, photocatalysis, and optoelectronic devices. The Fig.6.(b) shows the Tauc plot of MgO (magnesium oxide) nanoparticles, which is used to estimate the optical band gap energy (Eg) of the material. The Tauc plot is constructed by plotting $(\alpha h v)^2$ versus photon energy hv (in eV), assuming a direct allowed transition, which is typical for MgO. The linear portion of the curve is extrapolated to the energy axis (x-axis), and the point where it intersects gives the band gap energy. In this case, the extrapolation indicates a band gap of 3.14 eV. This band gap value is slightly lower than the bulk MgO band gap (~7.8 eV), which can be attributed to the nanoscale effects, particularly the presence of defects, oxygen vacancies, or quantum confinement in the nanoparticles. These effects introduce localized states within

the band gap or reduce the effective energy required for electronic transitions. The result confirms that MgO

nanoparticles exhibit semiconducting behaviour, making them suitable for applications in UV shielding,

photocatalysis, and optoelectronic devices where a tuneable band gap is beneficial.

Volume: 09 Issue: 11 | Nov - 2025

SJIF Rating: 8.586

ISSN: 2582-3930

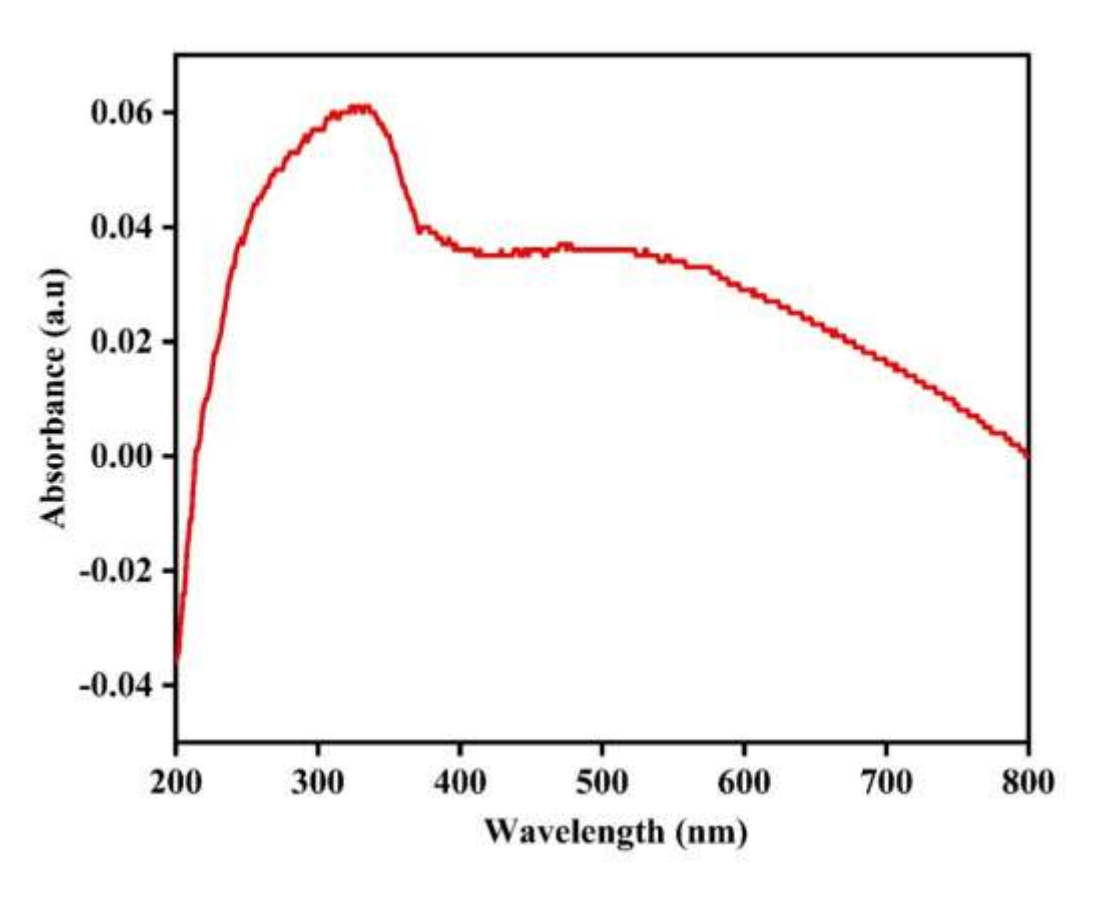
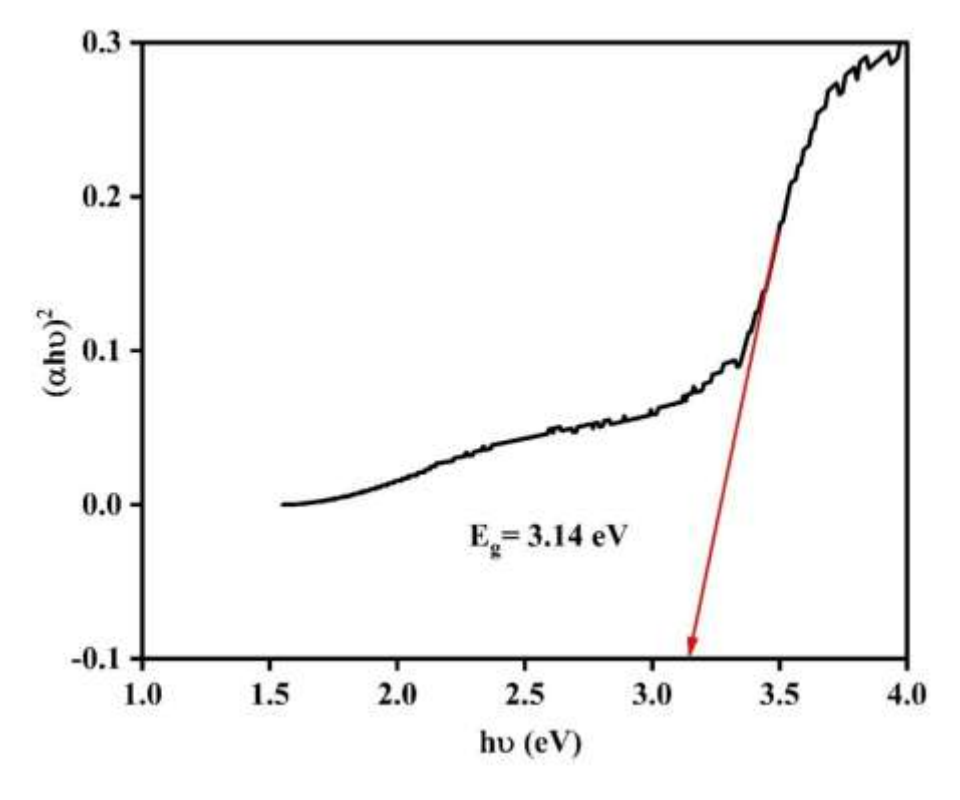


Fig.6. (a) UV-vis absorption plot of MgO NPs.



(b) Tauc's plot of MgO NPs.



Viscosity

Viscosity of the MgO–DI water nanofluids was measured using an Ostwald viscometer Fig.7. to evaluate the influence of nanoparticle concentration on the rheological behaviour of the fluid. Nanofluids with varying volume concentrations (0.020, 0.040, 0.060, 0.080, and 0.1 vol%) were prepared and maintained at a constant temperature during testing to ensure accuracy. The flow time of the nanofluid was recorded and compared with that of the base fluid (deionized water) to determine the relative viscosity. The increase in viscosity with nanoparticle concentration was attributed to enhanced particle–particle interactions and the formation of microstructures within the base fluid, indicating a deviation from Newtonian flow characteristics at higher concentrations. The viscosity values were calculated using the following equation [29] and are presented in the table 3.

$$\left(\frac{\mu_{nf}}{\rho_{nf}T_{nf}}\right) = \left(\frac{\mu_{bf}}{\rho_{bf}T_{bf}}\right) \tag{6}$$

Table.3. Viscosity of MgO - DI water Nanofluids.

Volume Concentration	Viscosity
(%)	(mPa·s)
0.020	0.83
0.040	0.90
0.060	0.89
0.080	0.94
0.100	0.97

Zeta potential

The stability of MgO nanofluids was evaluated by measuring the zeta potential using a Zetasizer Nano ZS (Malvern Instruments). The results for different volume concentrations (0.020–0.1 %) are summarized in Table, indicating good electrostatic stability of the nanofluids. The zeta potential values presented in table 4.

Volume: 09 Issue: 11 | Nov - 2025 SJIF Rating: 8.586

Table. 4. Zeta potential measurement of MgO - DI water Nanofluid.

Volume Concentration	Zeta Potential	Stability Interpretation
(%)	(mV)	
0.020	+43.2	Highly stable
0.040	+40.7	Stable
0.060	+37.5	Moderately stable
0.080	+36.2	Slightly stable
0.100	+29.8	Marginally stable

Thermal conductivity

The thermal conductivity of magnesium oxide (MgO) nanofluids is a critical parameter influencing their heat transfer performance. MgO nanoparticles dispersed in deionized water have been observed to enhance the base fluid's thermal conductivity due to the high intrinsic thermal conductivity of MgO and the increased effective surface area of nanoparticles. Thermal conductivity generally increases with nanoparticle concentration, as well as with temperature, due to intensified Brownian motion, micro-convection effects, and particle-fluid interactions. The values of thermal conductivity can be predicted using theoretical models such as the Maxwell model, volume concentrations (0.020-0.1 %) are summarized in Table which provides reasonable agreement with measured data for dilute nanofluids. Accurate measurement of thermal conductivity is essential for evaluating the potential of MgO nanofluids in applications such as cooling systems, heat exchangers, and energy-efficient thermal management. The thermal conductivity values presented in table 5.

The Maxwell equation is,[22, 30]

$$\frac{k_{nf}}{k_{bf}} = \frac{k_p + 2k_{bf} + 2\varphi(k_p - k_{bf})}{k_p + 2k_{bf} - \varphi(k_p - k_{bf})} \tag{7}$$

Table.5. Thermal conductivity of MgO - DI water Nanofluid.

Volume Concentration	Thermal Conductivity	Enhancement with DI water	
(%)	(W/m·K)	(%)	
0.000 (Base fluid – DI water)	0.598	_	
0.020	0.632	5.88 %	
0.040	0.665	11.99 %	



International Journal of Scientific Research in Engineering and Management (IJSREM)

Volume: 09 Issue: 11 | Nov - 2025 SJIF Rating: 8.586 **ISSN: 2582-3930**

0.060	0.704	18.36 %
0.080	0.747	24.99 %
0.100	0.783	31.90 %

Conclusion

Magnesium oxide (MgO) nanoparticles were successfully synthesized using the sol—gel method, which proved to be a simple, cost-effective, and efficient route for obtaining highly pure nanostructured materials. The XRD analysis confirmed the formation of crystalline MgO with a well-defined cubic phase structure. FTIR spectra revealed characteristic absorption bands corresponding to Mg—O vibrations, validating the formation of metal—oxygen bonds and confirming the purity of the synthesized nanoparticles. The UV—Vis analysis indicated strong optical absorption in the UV region, signifying a wide band gap and potential suitability for optical and photocatalytic applications. The MgO nanofluids prepared in deionized water exhibited enhanced thermal conductivity, which increased with nanoparticle concentration, indicating improved heat transfer potential. Viscosity measurements using an Ostwald viscometer showed a slight increase with particle loading, maintaining the fluid's suitability for practical applications. Zeta potential analysis demonstrated good colloidal stability across all concentrations, ensuring that the nanoparticles remained well-dispersed in the base fluid. Overall, the results confirm that the sol—gel technique is a promising approach for producing MgO nanoparticles with desirable structural, optical, and thermophysical properties suitable for environmental, catalytic, heat transfer, and energy-related applications.

Reference

- 1. Negrescu, A.M., et al., *Metal oxide nanoparticles: review of synthesis, characterization and biological effects.* Journal of Functional Biomaterials, 2022. **13**(4): p. 274.
- 2. Hornak, J., *Synthesis, properties, and selected technical applications of magnesium oxide nanoparticles: a review.* International Journal of Molecular Sciences, 2021. **22**(23): p. 12752.
- 3. Julkapli, N.M. and S. Bagheri, *Magnesium oxide as a heterogeneous catalyst support*. Reviews in Inorganic Chemistry, 2016. **36**(1): p. 1-41.
- 4. Chinthala, M., et al., *Synthesis and applications of nano-MgO and composites for medicine, energy, and environmental remediation: a review.* Environmental Chemistry Letters, 2021. **19**(6): p. 4415-4454.
- 5. Balakrishnan, G., et al., *Microstructure, optical and photocatalytic properties of MgO nanoparticles*. Results in Physics, 2020. **16**: p. 103013.
- 6. Mirza, F. and H. Makwana, *Synthesis and characterization of magnesium oxide (MgO) nanoparticles by Co-precipitation method.* J Innov Res Technol, 2021. **8**: p. 436-441.
- 7. Jeevanandam, J., Y.S. Chan, and M.K. Danquah, *Calcination-dependent morphology transformation of sol-gel-synthesized MgO nanoparticles*. ChemistrySelect, 2017. **2**(32): p. 10393-10404.
- 8. Hench, L.L. and J.K. West, *The sol-gel process*. Chemical reviews, 1990. **90**(1): p. 33-72.
- 9. Sutapa, I., et al. *Dislocation, crystallite size distribution and lattice strain of magnesium oxide nanoparticles.* in *Journal of Physics: Conference Series.* 2018. IOP Publishing.
- 10. Yousefi, S., B. Ghasemi, and M.P. Nikolova, *Morpho/Opto-structural characterizations and XRD-assisted estimation of crystallite size and strain in MgO nanoparticles by applying Williamson–Hall and size-strain techniques*. Journal of cluster science, 2022. **33**(5): p. 2197-2207.
- 11. Wu, P.-Y., et al., Comparative study on arsenate removal mechanism of MgO and MgO/TiO 2 composites: FTIR and XPS analysis. New Journal of Chemistry, 2016. **40**(3): p. 2878-2885.
- 12. Foster, M., M. Furse, and D. Passno, *An FTIR study of water thin films on magnesium oxide*. Surface science, 2002. **502**: p. 102-108.



13. Vogt, C., C.S. Wondergem, and B.M. Weckhuysen, *Ultraviolet-visible (UV-Vis) spectroscopy*, in *Springer handbook of advanced catalyst characterization*. 2023, Springer. p. 237-264.

- 14. Akash, M.S.H. and K. Rehman, *Ultraviolet-visible (UV-VIS) spectroscopy*, in *Essentials of pharmaceutical analysis*. 2019, Springer. p. 29-56.
- 15. Bindhu, M., et al., *Structural, morphological and optical properties of MgO nanoparticles for antibacterial applications*. Materials Letters, 2016. **166**: p. 19-22.
- 16. Nigam, A., et al., Structural, optical, cytotoxicity, and antimicrobial properties of MgO, ZnO and MgO/ZnO nanocomposite for biomedical applications. Ceramics International, 2021. 47(14): p. 19515-19525.
- 17. Giwa, S., et al., *Influence of nanoparticles size, per cent mass ratio, and temperature on the thermal properties of water-based MgO–ZnO nanofluid: An experimental approach.* Journal of Thermal Analysis and Calorimetry, 2021. **143**(2): p. 1063-1079.
- 18. Ilyas, S.U., et al., *Stability, rheology and thermal analysis of functionalized alumina-thermal oil-based nanofluids for advanced cooling systems*. Energy conversion and management, 2017. **142**: p. 215-229.
- 19. Angayarkanni, S. and J. Philip, *Review on thermal properties of nanofluids: Recent developments.* Advances in colloid and interface science, 2015. **225**: p. 146-176.
- 20. Choudhary, S., A. Sachdeva, and P. Kumar, *Investigation of the stability of MgO nanofluid and its effect on the thermal performance of flat plate solar collector.* Renewable Energy, 2020. **147**: p. 1801-1814.
- 21. Diez, R., et al., Development of nanofluids for the inhibition of formation damage caused by fines migration: effect of the interaction of quaternary amine (CTAB) and MgO nanoparticles. Nanomaterials, 2020. **10**(5): p. 928.
- 22. Pryazhnikov, M., et al., *Thermal conductivity measurements of nanofluids*. International Journal of Heat and Mass Transfer, 2017. **104**: p. 1275-1282.
- 23. Hassani, S.S., et al., *The effect of nanoparticles on the heat transfer properties of drilling fluids*. Journal of Petroleum Science and Engineering, 2016. **146**: p. 183-190.
- 24. Mukherjee, S., P. Chaudhuri, and P.C. Mishra, *Achieving Enhanced and Sustainable Thermo-Economic Performance with Aqueous MgO-SiO2 Hybrid Nanofluid under Controlled Mixing Ratio: Experimental Results.* Journal of Thermal Science, 2025. **34**(2): p. 429-447.
- 25. Beaulieu, L., et al., An automated system for performing continuous viscosity versus temperature measurements of fluids using an Ostwald viscometer. Review of Scientific Instruments, 2017. **88**(9).
- 26. Fatimah, S., et al., *How to calculate crystallite size from x-ray diffraction (XRD) using Scherrer method.* ASEAN Journal of Science and Engineering, 2022. **2**(1): p. 65-76.
- 27. Shintani, T. and Y. Murata, Evaluation of the dislocation density and dislocation character in cold rolled Type 304 steel determined by profile analysis of X-ray diffraction. Acta Materialia, 2011. **59**(11): p. 4314-4322.
- 28. Wani, S., et al., *Influence of chromium doping on structural, microstructure, optical and electrical properties of zinc ferrite.* Physica Scripta, 2024.
- 29. Mukherjee, S., et al., *Experimental investigation on thermo-physical properties and subcooled flow boiling performance of Al2O3/water nanofluids in a horizontal tube*. International Journal of Thermal Sciences, 2021. **159**: p. 106581.
- 30. Yu, W., Choi, and SUS, *The role of interfacial layers in the enhanced thermal conductivity of nanofluids: a renovated Maxwell model.* Journal of nanoparticle research, 2003. **5**(1): p. 167-171.